Grünthal, G., Stromeyer, D. (1992): The Recent Crustal Stress Field in Central Europe - Trajectories and Finite-element Modeling. - Journal of Geophysical Research, 97, B8, 11.805-11.820.

JOURNAL OF GEOPHYSICAL RESEARCH, VOL. 97, NO. B8, PAGES 11,805–11,820, JULY 30, 1992

The Recent Crustal Stress Field in Central Europe: Trajectories and Finite Element Modeling

G. GRÜNTHAL AND D. STROMEYER

Zentralinstitut für Physik der Erde, Potsdam, Germany

The recent crustal stress field of Central Europe and especially of the adjoining areas to the east is presented in terms of the directions of maximum horizontal stress ($S_{H\max}$). The analysis is based on fault plane solutions, in situ stress measurements, geologic fault slip determinations, and repeated precise geodetic triangulations. A bending of the direction of $S_{H\max}$ from the well-known NW-SE direction in the western part of the study area to directions of NE-SW to E-W in the eastern part is shown. First results on the recent crustal stress field of the study area were presented by Grünthal and Stromeyer (1986), who substantiated this tendency of bending in the central and eastern parts of the study area by few observations only. Therefore one aim of this paper was to compile observations on the areas with few data points. Generally, these additional data confirm the previously established pattern; in some areas, especially in the Pannonian basin, the stress features became more complicated compared with those solely based on a few data points. The second part of the paper presents steady state elastic finite element model calculations to provide some possible explanations of the observed stress orientations as a result of plate driving forces. Simulation of the North Atlantic seafloor spreading and the northward directed motion of the African plate by appropriate boundary loads produces a pattern of $S_{H\max}$ directions for the western part of the Eurasian plate which is compatible with the broad-scale observed stress directions. Subregional anomalies such as the fanlike stress pattern perpendicular to the arc of the Western Alps or the radial directions around the Pannonian basin can be explained only when additional stress producing features are introduced overmodulating the regional field. Rigorous introduction of physically constrained model parameters for all these features was not feasible to date. Therefore the preliminary empirical model calculations presented in this paper are attempts to discuss which features have the most influence on the stress field. They are, in a regional scale, the North Atlantic seafloor spreading, the northward motion of the African and the Arabian plate, and obviously, subregionally, increased stiffness of the Apulian promontary as well as of the Bohemian massif.

1. INTRODUCTION

In this paper we present an update of the *Grünthal and Stromeyer* [1986] compilation of stress orientation data and their finite element modeling for Central Europe. The term Central Europe is used here in a broader sense. We have chosen our area of special interest that it includes the following remarkable tectonic features: (1) the Alpine mountain chains of the entire Alps and the entire Carpathians, (2) the seismically active Upper Rhine Graben and the Lower Rhine embayment, and (3) parts of the Variscan West European platform separated by the Tornquist-Teysseire line from the East European platform. The area, on which we focused our research activities, reaches from 44°N to 54°N and from 3°E to 30°E.

Previously, we found that the crustal stress state of Central Europe, in terms of its horizontal compressive component, generally has regional uniformity. The data available for the eastern half of the study area, being relatively scarce in this paper, show a tendency following a stress direction of NE-SW to east-west. This pattern differs considerably from the well-established NW-SE to NNW-SSE direction in western Central Europe, that is, especially the Western Alps and the Rhine area, which is based both on orientations of maximum horizontal stress $S_{H\max}$ of in situ stress measurements (overcoring or hydrofrac), for example, after *Illies et al.* [1981] or *Baumann and Illies* [1983], and on directions of P axes of earthquake fault plane solutions, for example, by *Ahorner et al.* [1983] or by *Pavoni* [1980*a*].

The observed broad-scale stress pattern, which is primarily tectonic in origin [*Zoback et al.*, 1989], was found in our previous paper to be in agreement with rather simple numerical stress field calculations for a homogeneous elastic plate under boundary loads according to plate tectonic driving forces. The finite element procedure used here relies on an improved model, but regarding the complexity of the problem to be solved, this approach constrains strongly simplified assumptions.

The aims of this study are (1) to complete our presently relatively limited knowledge on the state of stress in the central, eastern, and southeastern parts of the study area, that is, the stable and therefore aseismic or low seismicity parts of the Variscan European platform, parts of the East European platform, the Pannonian basin, and the Carpathian belt and (2) to provide to an explanation of the observed stress pattern using an elastic finite element modeling of the Earth's crust in the western part of the Eurasian plate reaching up to the plate boundaries in the North Atlantic and in the Mediterranean region.

2. DATA

Up to now the only stress parameter for the Earth's crust which is available with sufficient reliability and in sufficient quantity is the direction of principal stress. Usually, projection on the Earth's surface is used for simplifying the approach. So, all our considerations are restricted to horizontal compressive and tensional stress directions assumed to be representative for the Earth's crust.

Paper number 91JB01963.
0148-0227/92/91JB-01963$05.00

This study is generally based on published stress data compiled by the authors; some previously unpublished stress data have been added (e.g., data taken from special research reports or from personal communications). All data in this paper are quality ranked according to the World Stress Map project and are included in the World Stress Map data base available on floppy disks from the National Geophysical Data Center, Boulder, Colorado (see *Zoback* [this issue] for details). Some published data which were assessed and turned out to be too poor were deleted from our data set. According to the above mentioned restriction of our contribution to the study of the directions of horizontal stresses, we do not consider the magnitudes of the stress components in the different tabulated compilations discussed below. The appropriate stress magnitude information is included in the data base of the World Stress Map.

Most stress information results from earthquake focal mechanism solutions. We utilized focal mechanism data for single events, composite solutions, and, in a few cases, averages of focal mechanisms with appropriate quality ranking. Only crustal earthquakes were considered. If the same focal mechanism solution for an earthquake was published by different authors, we refer to the earliest paper. In the case where different solutions exist for the same earthquake we select the best constrained mechanism, that is, the solution which is based on the largest number of polarity readings or for which better reliability criteria can be given as compared with other solutions. In agreement with the editorial board of this issue we restrict the data presentation to the region east of 10°E (Table 1), the area especially covered by this paper as described in the introduction. The data for western Europe are described in detail by *Müller et al.* [this issue]. All data are available on floppy disks as previously mentioned.

Another type of data of principal stress orientations is derived from in situ stress measurements (hydrofrac and overcoring and to this group we also refer to the technique of analyzing drill hole elongations). Following the general policy of this special section, previously published in situ stress data are not given here in tabulated form, unless those data are from generally inaccessible publications. Also, those in situ stress data which were already included in the data file of the World Stress Map Project and which are the focus of *Müller et al.* [this issue] are not repeated here. Additionally, the restriction on data east of 10°E holds also for this data set. The remaining in situ stress data are compiled in Table 2.

Some of the tabulated in situ stress data [*Gross*, 1989] are from the North German plain, a sedimentary basin reaching a sediment thickness of up to 10 km. For our study we consider only those stress data of this region from depths beneath the base of the Zechstein-salthorizon (in the area studied by *Gross* [1989] in a depth range of 3100–3300 m) because the stress data above this horizon are mainly influenced by salt domes representing strong lateral inhomogeneities. Simple model considerations show that salt domes cause extreme changes of the direction of the stress field near to such diapirs [*Schneider*, 1985]. Changes of stress directions with depth are known also from other sedimentary basins (for example, by *Becker et al.* [1984] for northern Switzerland). Generally, in this study we use the data from the greatest depths when data from different depths for one locality are available and especially when changing stress directions with depth are observed.

The third and fourth types of data used in this study are stress directions inferred from geologic fault slip and principal strain directions inferred from repeated geodetic triangulations (see Table 3 for data east of 10°E). These data are described briefly.

Poljak [1984] measured trends of several tens of extensional and shear fractures as well as fold axes at different outcrops in the Mur depression (northernmost Yugoslavia, SW margin of the Pannonian basin) and inferred $S_{H\max}$ orientations from trends of these different features as represented on Schmidt diagrams. The analysis of the structural neotectonic (post-Pliocene) elements shows NE-SW compression (events 7 and 8 in Table 3). Other post-Oligocene and post-Miocene data of Poljak's paper were not used in our investigation which is focused, like the World Map Project, on youngest stress conditions.

Kotas [1983] describes (Pleistocene-Holocene) strike-slip offsets on a family of faults in central and southern parts of Poland. These offsets occur as dextral movements on N-S trending faults in central Poland and as dextral movements on N-S faults and sinistral movements on conjugate E-W oriented faults in southern Poland. According to classical frictional faulting theory the maximum compression axis can be assumed at about 30° to the N-S faults in central Poland; however, the $S_{H\max}$ direction for the near-perpendicular conjugate faulting in southern Poland is taken as the bisector or suggesting a mean NE-SW $S_{H\max}$ direction (45°).

Pilarski [1988] interpreted $S_{H\max}$ directions in eastern Saxony from combined analysis of satellite images and field observations at several sites. He found N-S directed joints in outcrops of glacial deposits of the Saalian ice age (0.1–0.2 Ma). The extensional character of the N-S elements is evident. Some of these joints are connected with NNE elements, both form wedge-shaped configurations. The N-S elements are related to small strike-slip offsets and $S_{H\max}$ should be N30°–45°E.

Geodetically derived directions θ_1 of maximum horizontal compressional strain are also tabulated in Table 3. According to *Thurm et al.* [1977], θ_1 follows from the shear strain γ, using $\theta_1 = 1/2 \arctan [\gamma/(\varepsilon_x - \varepsilon_y)]$, where ε_x is the strain component in N-S direction and ε_y is the strain component in E-W direction.

Strain data were analyzed by *Thurm et al.* [1977] for an area of 12500 km^2 (Saxony) based on triangulations carried out in 1890 and 1960. The different strain parameters were computed for 880 points of this study area and depicted in maps. Despite some local derivations, the clear majority of data shows a dominating NW-SE directed compression. We have tabulated this mean value, recognizing that it represents a principal strain, but principal stress, direction. Strain data are included here because they provide additional information on the deformation of the crust and, assuming an isotropic relationship between stress and strain, they can be interpreted in the context of the stress data. Similarly, this type of data was determined in Czechoslovakia by *Vyskocil* [1985, 1987] but with a less dense net of data points. The triangulation data do not have a quality assigned since the qualities based on the standards of the World Stress Map Project are not defined for these data.

Stress patterns determined by in situ techniques usually show a striking correspondence with data obtained by fault

TABLE 1. Stress Orientation Data From Focal Mechanism Studies

No.	Latitude °N	Longitude °E	Date	M	Depth, km	Q	Type	P Axis Strike, deg	P Axis Dip, deg	T Axis Strike, deg	T Axis Dip, deg	Reference
1	48.55	10.2	May 17, 1982			C	FMS	345.	30.	248.	15.	*Schmedes* [1987]
2	44.23	10.20	Oct. 15, 1939	4.9	26.	C	FMS	118.	26.	96.	10.	*Cagnetti et al.* [1976]
3	44.78	10.29	July 15, 1971	4.8	7.	C	FMS	333.	56.	184.	30.	*Gasparini et al.* [1985]
4	44.80	10.30	July 15, 1971	5.3	8.	B	FMS	12.	35.	277.	10.	*Cagnetti et al.* [1976]
5	47.16	10.75	1965			D	FMA	174.				*Schneider* [1967]
6	47.45	10.78	Oct. 8, 1930	5.4		C	FMS	221.	07.	316.	47.	*Cagnetti et al.* [1976]
7	44.14	10.80	Jan. 6, 1969	4.1		C	FMS	314.	60.	171.	25.	*Gasparini et al.* [1985]
8	48.37	10.88	Aug. 2, 1981	3.1	28.	C	FMS	353.	48.	257.	7.	*Schmedes* [1984]
9	44.07	11.64	Feb. 11, 1939	4.7	7.	C	FMS	150.	74.	241.	1.	*Gasparini et al.* [1985]
10	44.41	11.99	Dec. 5, 1978	4.6	18.	C	FMS	317.	60.	214.	8.	*Gasparini et al.* [1985]
11	44.63	12.01	Dec. 30, 1967	5.2		C	FMS	49.	11.	248.	79.	*Gasparini et al.* [1985]
12	46.1	12.3	Oct. 18, 1936	5.6		C	FMS	162.	24.	64.	18.	*Ahorner et al.* [1972]
13	50.25	12.45	Jan. 24, 1986	2.4		C	FMS	137.	38.	263.	38.	*Zahradnik et al.* [1988]
14	50.25	12.45	Feb. 6, 1986	2.4		C	FMS	130.	42.	257.	33.	*Zahradnik et al.* [1988]
15	50.25	12.45	Jan. 24, 1986	2.0		D	FMS	132.	47.	260.	29.	*Zahradnik et al.* [1988]
16	50.25	12.45	Jan. 21, 1986	1.8		D	FMS	109.	42.	251.	42.	*Zahradnik et al.* [1988]
17	50.24	12.45	Dec. 24, 1985	3.9		C	FMS	117.	52.	224.	12.	*Grosser and Köhler* [1988]
18	50.24	12.45	Dec. 21, 1985	4.0		B	FMS	119.	42.	20.	9.	*Grosser and Köhler* [1988]
19	50.24	12.45	Dec. 16, 1985	3.2		C	FMS	127.	5.	246.	79.	*Grosser and Köhler* [1988]
20	50.24	12.45	Dec. 25, 1985	2.4		C	FMS	147.	11.	243.	30.	*Antonini* [1988]
21	50.24	12.45	Dec. 23, 1985	4.0		B	FMS	328.	3.	236.	36.	*Antonini* [1988]
22	50.24	12.45	Jan. 7, 1986	2.3		D	FMS	148.	36.	44.	18.	*Antonini* [1988]
23	50.24	12.45	Dec. 30, 1985	2.8		C	FMS	143.	27.	234.	2.	*Antonini* [1988]
24	50.24	12.45	Dec. 18, 1985	2.4		C	FMS	166.	43.	67.	10.	*Antonini* [1988]
25	50.24	12.45	Dec. 21, 1985	4.6		B	FMS	127.	32.	223.	9.	*Antonini* [1988]
26	50.25	12.45	Jan. 20, 1986	4.2		B	FMS	146.	0.	56.	0.	*Antonini* [1988]
27	50.23	12.46	Jan. 24, 1986	2.0		D	FMS	111.	48.	255.	36.	*Zahradnik et al.* [1988]
28	50.23	12.46	Jan. 7, 1986	1.9		D	FMS	119.	42.	261.	42.	*Zahradnik et al.* [1988]
29	46.0	12.5	Oct. 19, 1936	4.5	10.	C	FMS	159.	00.	69.	00.	*Ritsema* [1974]
30	46.3	12.5	June 8, 1934	4.5	20.	C	FMS	160.	0.	70.	0.	*Ritsema* [1974]
31	50.61	12.69				D	FMC	148.8	25.2	248.4	19.4	H. Konietzky (personal communication, 1989)
32	46.56	12.96	Nov. 5, 1956	4.8	2.	C	FMS	315.	2.	45.	2.	*Cagnetti et al.* [1976]
33	46.4	13.0	March 27, 1928	5.8	20.	C	FMS	351.	8.	131.	78.	*Ritsema* [1974]
34	46.42	13.03	March 27, 1928	5.8	20.	C	FMS	355.	10.	263.	35.	*Cagnetti et al.* [1976]
35	47.00	14.20	June 1, 1969	4.5		B	FMS	143.	6.	53.	25.	*Cagnetti et al.* [1976]
36	47.91	14.26	Jan. 29, 1967	4.6	22.	B	FMS	25.	63.	190.	26.	*Cagnetti et al.* [1976]
37	47.60	15.80	Oct. 27, 1964			C	FMS	228.	6.	323.	35.	*Gangl* [1975]
38	47.60	15.80	June 30, 1964			C	FMS	45.	11.	126.	02.	*Gangl* [1975]
39	47.73	15.92	June 30, 1964		3.	C	FMS	47.	0.	137.	0.	*Ritsema* [1974]
40	47.85	15.95	Oct. 27, 1964		1.	C	FMS	196.	36.	301.	20.	*Ritsema* [1974]
41	47.73	16.02	April 16, 1972		19.	C	FMS	5.	8.	100.	27.	*Ritsema* [1974]
42	47.72	16.07	April 16, 1972			C	FMS	352.	14.	82.	0.	*Gangl* [1975]
43	51.46	16.14	June 20, 1987	2.1	0.8	D	FMS	186.0	33.0	84.0	82.0	*Gibowicz et al.* [1989]
44	51.45	16.15	July 11, 1987	2.1	0.8	D	FMS	188.0	19.0	96.0	89.0	*Gibowicz et al.* [1989]
45	51.46	16.15	June 24, 1987	1.9	0.8	D	FMS	191.0	27.0	81.0	80.0	*Gibowicz et al.* [1989]
46	47.73	16.15	April 16, 1972			C	FMS	147.	40.	224.	08.	*Gangl* [1975]
47	48.03	16.20	Dec. 2, 1963			C	FMS	90.	25.	270.	65.	*Ritsema* [1974]
48	50.86	16.20	1979			C	FMC	253.	66.	39.	15.	*Gibowicz and Cichowicz* [1986]
49	47.80	16.25	Jan. 5, 1972			C	FMS	191.	0.	101.	15.	*Gangl* [1975]
50	46.2	16.8	March 27, 1938	5.6	7.	C	FMS	40.	35.	220.	55.	*Ritsema* [1974]
51	44.98	17.04	Oct. 27, 1969		18.	C	FMS	15.	5.	195.	85.	*Ritsema* [1974]
52	44.85	17.22	Oct. 27, 1969	6.1		C	FMS	196.	10.	298.	51.	*Ritsema* [1974]
53	44.88	17.23	Dec. 31, 1969			C	FMS	28.	50.	277.	16.	*Ritsema* [1974]
54	44.85	17.23	Oct. 26, 1969			C	FMS	190.	13.	100.	01.	*Gangl* [1975]
55	44.84	17.30	Oct. 26, 1969	5.6		C	FMS	194.	23.	333.	60.	*Ritsema* [1974]
56	45.27	18.04	April 13, 1964	6.1	5.	B	FMS	62.	9.	290.	76.	*Cagnetti et al.* [1976]
57	47.06	18.1	Aug. 15, 1985	4.7	10.	C	FMS	85.4	21.8	355.1	0.6	*Monus et al.* [1988]
58	45.30	18.17	April 13, 1964			C	FMS	29.	06.	123.	31.	*Gangl* [1975]
59	48.74	19.16	March 4, 1978			D	FMS	68.				*Pospisil et al.* [1985]
60	47.5	19.3	Jan. 12, 1956	5.7		C	FMS	143.	0.	53.	66.	*Ritsema* [1974]
61	51.25	19.40	Nov. 12, 1980	4.6	2.	C	FMS	64.	15.	328.	19.	*Gibowicz et al.* [1982]
62	46.75	21.13	June 22, 1978	3.9		D	FMS	221.8	33.5	120.9	16.	*Monus et al.* [1988]
63	46.75	21.13	June 22, 1978	4.6	8.	D	FMS	28.8	11.7	130.0	43.1	*Monus et al.* [1988]
64	48.48	22.23	July 1, 1982	4.6	3.	C	FMS	225.7	5.5	86.9	82.7	*Monus et al.* [1988]
65	47.68	23.22	March 30, 1979	4.7		C	FMS	94.				*Polonic* [1985]
66	47.82	23.31	March 8, 1979	3.9		C	FMS	92.		5.		*Polonic* [1985]
68	45.3	25.1	April 18, 1969	5.2	10.	B	FMS	90.	26.	188.	16.	*Oncescu* [1987]

TABLE 1. (continued)

No.	Latitude °N	Longitude °E	Date	M	Depth, km	Q	Type	P Axis Strike, deg	P Axis Dip, deg	T Axis Strike, deg	T Axis Dip, deg	Reference
70	45.1	26.	Feb. 8, 1975	4.7	23.	B	FMS	275.	3.	7.	26.	*Oncescu* [1987]
71	45.9	26.6	March 7, 1975	5.1	21.	B	FMS	6.	16.	104.	26.	*Oncescu* [1987]
72	45.7	26.8	June 3, 1952	4.5	22.	D	FMS	116.	6.	224.	71.	*Ritsema* [1974]
73	45.4	26.9	Dec. 23, 1957		25.	D	FMS	238.	70.	112.	8.	*Radu* [1976]
74	47.9	26.9	July 10, 1970			C	FMS	280.	16.	113.	74.	*Radu* [1976]
76	45.47	27.08	April 27, 1986	5.0	19.0	C	FMS	128.	2.	229.	82.	*Oncescu and Trifu* [1987]
77	45.3	27.1	Feb. 21, 1983	4.5	19.	B	FMS	311.	16.	178.	67.	*Oncescu* [1987]
78	45.3	27.1	March 5,1977	4.3	10.	B	FMS	233.	22.	336.	28.	*Oncescu* [1987]
79	45.5	27.1	April 27, 1986	5.	26.	B	FMS	128.	2.	229.	82.	*Oncescu* [1987]
80	44.4	27.2	Dec. 8, 1980	4.	15.	C	FMS	96.	29.	205.	31.	*Oncescu* [1987]
81	45.89	27.39	May 31, 1959	5.2		C	FMS	55.	45.	235.	45.	*Ritsema* [1974]
82	46.1	27.4	April 18, 1956		20.	D	FMS	265.	30.	52.	55.	*Radu* [1976]
83	45.4	28.2	Sept. 11, 1980	4.7	15.	B	FMS	237.	1.	147.	1.	*Oncescu* [1987]
84	45.2	29.	Nov. 13, 1981	5.2	10.	B	FMS	60.	9.	175.	69.	*Oncescu* [1987]

Types of indicators: FMS, single solution; FMC, composite solution; FMA, average of focal mechanisms. Q, quality ranking (according to the notation of the World Stress Map Project).

plane solutions of earthquakes. *Ahorner* [1985] compared direction diagrams of the P axis of earthquake fault plane solutions with $S_{H\max}$ axes of in situ measurements (Figure 1) of western Central European data. Their congruence is noteworthy and encouraged us to use both data sets for this study without restrictions, provided they are good quality solutions. The identification of the P axis with the $S_{H\max}$ axis is based on the thesis that the shear angle between the slip and the direction of principal compressive stress is 45°. But laboratory measurements frequently show this angle to be closer to 30° which would result in a possible error of the data derived from fault plane solutions of about 15°. In fact, comparison between the two different data sets of other parts of the world [see *Zoback and Zoback*, 1980*a*, *b*] does not confirm such errors, but one can state that on average the directions of P axes can be taken to coincide with the axis of maximum compression. For further discussions on the problems of the correlation between earthquake P and T axes, nearby in situ stress data, as well as stress directions inferred from geological observations, we refer, for example, to *Zoback* [1989] or to *Zoback and Zoback* [1980*a*, *b*].

Figure 2 shows all compiled $S_{H\max}$ directions within the area under study. A special detailed compilation of data for the Western Alpine arc is given in Figure 3.

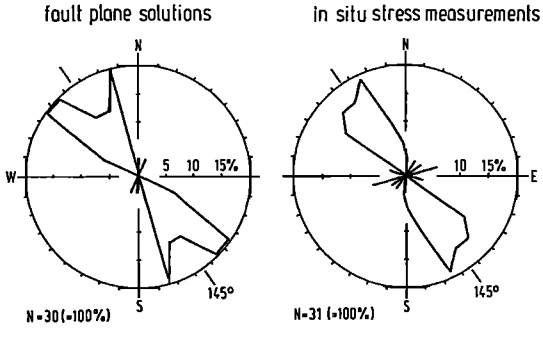

Fig. 1. Comparison of relative direction frequencies of maximum horizontal compressive stress in Central Europe [after *Ahorner*, 1985] determined from (1) directions of pressure axes of earthquake fault plane solutions (left) and from (2) directions of $S_{H\max}$ axes of in situ stress measurements (right).

In comparison to *Grünthal and Stromeyer* [1986] the previously available numerous observations for western Central Europe, especially for the Rhine area and in the Swiss Jura Mountains, were enhanced by additional data (for references see caption of Figure 2) which confirm the previous patterns. For our previous study we collected a few stress indications in the region adjoining to the East European platform showing stress directions which are basically different from the well-established direction in western Central Europe. Therefore the special aim of this study was to improve our limited knowledge about the crustal stress conditions of the region eastward of western Central Europe with its well-documented features. We have increased the contemporary stress data set for Poland, Hungary, and Romania. Other useful new data were also added for northern Yugoslavia, Czechoslovakia, eastern parts of Germany, and Bavaria. No new data could be added for the portion of the East European platform under study in this paper.

3. STRESS TRAJECTORIES

All observations, compiled in Tables 1–3 and depicted in Figures 2 and 3, respectively, were visually averaged and generalized in form of trajectories of the maximum horizontal compressive stress (Figure 4). Additionally, Figure 4 contains some first-order tectonic information, as main first-order tectonic faults and indications for extensional regimes in the crust.

The dominant features of the compressive stress trajectories depicted in Figure 2 are as follows: (1) a well-established NW-SE directed compression in western Central Europe, (2) a fanlike pattern of compressive stresses at right angles to the arc of the Western Alps or, in other words, normal to the alpidic striking [*Pavoni*, 1975], (3) a clockwise change in $S_{H\max}$ orientation to SW-NE along the margin of the East European platform, (4) extensional deformation within the Pannonian basin, and (5) further clockwise change of $S_{H\max}$ to E-W and WNW-ESE east of the Pannonian basin. This change in $S_{H\max}$ orientation, compared to the NW-SE pattern dominant in western Central Europe, seems to start (from west to east) at the southern margins of the North German plain, within the Bohemian massif, and within the

TABLE 2. Stress Orientation Data From Overcoring (OC), Hydrofrac (HF), and Breakout (BO) Measurements

No.	Latitude °N	Longitude °E	Type	Depth, m	S_{Hmax}, deg	Quality	Reference
1	50.79	10.00	HF	808	148	D	*Knoll* [1979]
2	51.84	10.27	HF	60–226	101	B	*Rummel and Baumgärtner* [1982]
3	46.18	10.35	OC	250	148	D	*Martinetti and Ribacchi* [1980]
4	46.06	10.35	OC	240	150	C	*Martinetti and Ribacchi* [1980]
5	51.78	10.79	OC	400	160	B	*Knoll* [1979]
6	52.67	11.00	HF	3200	18	A	*Gross* [1989]
7	49.96	11.08	OC	0	134	C	*Kraft* [1984]
8	49.87	11.18	OC	0	146	D	*Kraft* [1984]
9	44.85	11.20	BO		160	C	*Cox* [1983]
10	50.26	11.36	OC	0	143	C	*Cox* [1983]
11	50.25	11.39	OC	0	156	C	*Cox* [1983]
12	49.73	11.45	OC	0	155	C	*Cox* [1983]
13	50.24	11.46	OC	0	139	D	*Cox* [1983]
14	49.81	11.51	OC	0	131	C	*Cox* [1983]
15	49.77	11.54	OC	0	165	C	*Cox* [1983]
16	49.96	11.66	OC	70	133	B	*Cox* [1983]
17	50.13	11.69	HF	55–73	143	D	*Rummel and Baumgärtner* [1982]
18	50.14	11.86	OC	2–3	4	B	*Wolter* [1987]
19	50.13	11.87	OC	0	172	D	*Wolter* [1987]
20	50.12	11.90	OC	0	150	D	*Wolter* [1987]
21	49.91	11.93	OC	0	140	D	*Kraft* [1984]
22	49.90	11.94	OC	0	53	D	*Kraft* [1984]
23	49.83	12.12	BO		103	A	*Becker and Paladini* [1990]
24	50.05	12.15	HF	64–122	138	B	*Rummel and Baumgärtner* [1987]
25	49.86	12.20	HF	81–288	96	B	*Rummel and Baumgärtner* [1982]
26	49.99	12.20	OC	0	119	D	*Kraft* [1984]
27	49.83	12.28	HF	104–156	117	D	*Rummel and Baumgärtner* [1982]
28	46.44	12.42	OC	120	76	C	*Martinetti and Ribacchi* [1980]
29	49.21	12.48	OC	30	32	D	*Carniel and Roch* [1976]
30	49.87	12.50	HF	24–227	163	B	*Rummel and Baumgärtner* [1987]
31	46.55	12.62	OC	280	23	D	*Martinetti and Ribacchi* [1980]
32	50.60	12.72	OC	1500	165	B	*Knoll* [1979]
33	50.46	13.03	OC	400	160	D	*Knoll* [1979]
34	50.70	13.05	OC		135	D	*Mjakischev* [1983]
35	50.91	13.33	OC		168	D	*Mjakischev* [1983]
36	46.44	13.57	OC	400	93	C	*Martinetti and Ribacchi* [1980]
37	46.63	13.65	OC	560	109	C	*Kohlbeck et al.* [1980]
38	46.63	13.68	OC	236	119	C	*Kohlbeck et al.* [1980]
39	50.77	13.87	OC		158	D	*Mjakischev* [1983]
40	46.93	14.57	OC	120	106	C	*Hermann et al.* [1983]
41	47.19	14.69	OC	1100	7	B	*Kohlbeck* [1979]
42	47.28	15.17	OC	800	142	B	*Kohlbeck et al.* [1984]
43	46.77	16.33	BO		102	B	B. Müller and F. Horvath (unpublished data, 1989)
44	48.13	16.92	OC	2.0–4.4	115	C	*Becker* [1985]
45	47.33	17.65	BO		124	B	B. Müller and F. Horvath (unpublished data, 1989)
46	46.70	19.92	BO		37	C	B. Müller and F. Horvath (unpublished data, 1989)
47	46.25	20.03	BO		79	D	B. Müller and F. Horvath (unpublished data, 1989)
48	46.68	20.45	BO		7	C	B. Müller and F. Horvath (unpublished data, 1989)
49	46.87	20.62	BO		113	C	B. Müller and F. Horvath (unpublished data, 1989)
50	47.20	21.32	BO		152	D	B. Müller and F. Horvath (unpublished data, 1989)
51	47.37	21.70	BO		116	B	B. Müller and F. Horvath (unpublished data, 1989)
52	47.80	22.08	BO		100	C	B. Müller and F. Horvath (unpublished data, 1989)

Data are for the region 10°E to 30°E and 44°N to 54°N.

northern Dinaric Alps (south of the Pannonian basin). When drawing the trajectories from north to south with more or less equal spacing of starting points, inevitably the spacings between the single lines are decreasing steadily when continuing southward. The highest density of trajectories occurs within the Alps perpendicular to the Alpine arc. There arises the question of whether this increasing density of trajectories toward the Alps may be linked to the increasing absolute values of horizontal compressive stress towards the Alps (from north to south) determined at 14 sites by means of the doorstopper method by *Baumann and Illies* [1983].

Some regional details of the derived stress pattern of Central Europe in a broader sense (Figure 4) can be described as follows:

Upper Rhine Graben, Lower Rhine Embayment, and Western Alps

The clear NW-SE compression in the Rhine area seems to be deflected due to active shear strain along the Rhine Graben rift and due to active tensile forces [e.g., *Ahorner*, 1975; *Baumann and Illies*, 1983] between Lower Rhine embayment and Upper Rhine Graben. This deflection is manifested in a anticlockwise bending of the trajectories.

TABLE 3. Stress Direction Data From Geological Observations (GFS) and Geodetic Measurements (TRIA)

No.	Latitude °N	Longitude °E	Type	Stress Regime	Q	S_{Hmax}, deg	Reference
1	50.2	12.7	TRIA			114.	*Vyskocil* [1987]
2	50.8	13.0	TRIA			145.	*Thurm et al.* [1977]
3	50.4	13.1	TRIA			104.	*Vyskocil* [1987]
4	50.4	13.7	TRIA			148.	*Vyskocil* [1987]
5	51.66	14.24	GFS	N	D	30.	*Pilarski* [1988]
6	49.0	14.5	TRIA			30.	*Vyskocil* [1985]
7	46.9	16.0	GFS	SS/T	C	30.	*Poljak* [1984]
8	46.6	16.3	GFS	SS/T	C	46.	*Poljak* [1984]
9	48.9	16.4	TRIA			30.	*Vyskocil* [1985]
10	52.7	17.8	GFS	SS	C	30.	*Kotas* [1983]
11	50.5	19.8	GFS	SS	C	45.	*Kotas* [1983]

Data are for the region 10°E to 30°E and 44°N to 54°N; Q, quality ranking; N, normal faulting; SS/T, strike slip with thrust component; and SS, pure strike slip.

The broadscale tectonic stress field within the Alps and its foreland is probably superimposed by more localized sources of tectonic stress, such as the topographic stresses (caused by the mean elevation of the Alps of about 2000 m over their foreland), by the buoyancy of their root, and by an anisotropy of strength or elastic properties of the lithosphere. Obviously, the buoyancy forces do not dominate in the Alps because deviatoric tension beneath the Alpine mountain range is not typical for this region.

The fanlike stress pattern perpendicular to the arc of the Western Alps and Jura Mountains (Figure 3) may be explained by the cold, dense, and slowly subsiding lithospheric root beneath the mountain chain [*Müller*, 1984]. Such a negative buoyancy induces compressive stresses directed

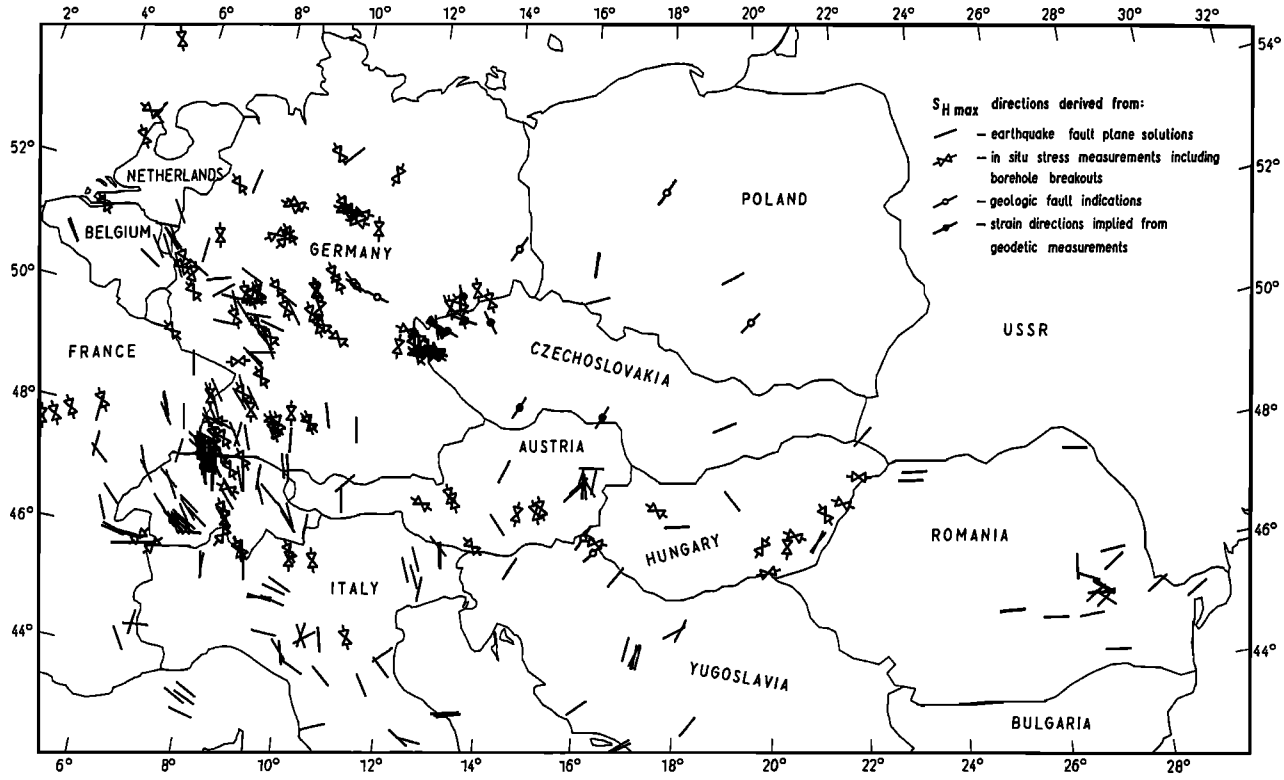

Fig. 2. Directions of maximum horizontal compression stress in the Earth's crust of Central Europe in a broader sense. Besides the data given in Tables 1–3, data are from *Ahorner* [1985], *Ahorner et al.* [1972, 1983], *Ahorner and Murawski* [1975], *Ahorner and Pelzing* [1983], *Ahorner and Schneider* [1974], *Bonjer et al.* [1984], *Cagnetti et al.* [1976], *Dorel et al.* [1983], *Gasparini et al.* [1985], *Hiller* [1936], *Hinzen* [1984], *Jimenez and Pavoni* [1984], *Leydecker et al.* [1980], *Neugebauer and Tobias* [1977], *Pavoni and Peterschmidt* [1974], and *Pavoni* [1980*a*, *b*] for earthquake P axes and from *Baumann and Illies* [1983], *Baumgärtner et al.* [1987], *Becker* [1985], *Blümling* [1986], *Blümling et al.* [1983], *Greiner and Illies* [1977], *Greiner* [1975], *Rummel and Ahlheid* [1980], and *Rummel et al.* [1983] for in situ measurements.

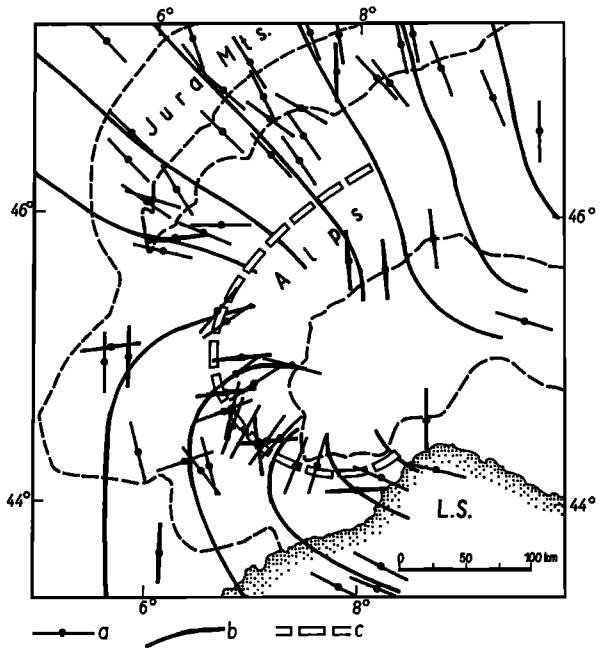

Fig. 3. Crustal stress field as determined from the focal mechanisms of earthquakes in the Western Alpine arc and in the Jura Mountains (redrawn, extended, and modified after *Pavoni* [1975], supplemented by data compiled by *Philip* [1980] and *Pavoni* [1986] and by the data listed in Table 1). The a curves are *P* axes of earthquake focal mechanisms; b curves are trajectories of maximum horizontal compressive stress (modiifed and extended after *Pavoni* [1975]; the c curves are the arc of the Western Alps; LS, Ligurian Sea.

toward the anomaly. This nearly vertical zone of a cold dense upper mantle root under the Alps, interpreted from several sets of geophysical data, penetrates to depths of about 100–200 km [*Müller*, 1984]. Additionally, the fanlike stress pattern in the Western Alps seems to be in agreement with *Laubscher*'s [1988] push-arc model. According to his model the Adriatic promontory or Adriatic plate is, in addition to its NNW tending compressive thrust, also pushed as an indenter at least with its northwesternmost branch, westward into the European plate, resulting in a continent-continent collision. This has been schematically outlined in Figure 6. For more details in discussing the stress conditions in western Central Europe we refer to *Müller et al.* [this issue].

North German Plain and NE Margin of the West European Platform

Obviously, the stress data available for Poland and northern eastern Germany indicate different $S_{H\max}$ orientations compared with the well-established NW-SE direction in western Central Europe. All $S_{H\max}$ data for Poland and northeastern Germany are oriented NNE-SSW or NE-SW. This pattern is derived from hydrofrac data (northeasternmost point in Germany) an A quality measurement at a depth of more than 3000 m (see Table 2), from fault plane solutions after *Gibowicz and Cichowicz* [1986] and *Gibowicz et al.* [1982, 1989] of relatively weak events (therefore in part D quality events), and from slip directions on faults [*Kotas*, 1983]. Also several $S_{H\max}$ data from hydraulic fracturing in southern Sweden (of A and B quality) show this NNE-SSW or NE-SW direction [*Müller et al.*, this issue], while earthquake *P* axes indicate NW-SE directions [*Slunga et al.*, 1984].

The NE-SW pattern seems to change in the western part of the North German plain. Numerous breakout measurements carried out there (see also *Müller et al.* [this issue]) indicate clearly the NW-SE direction of $S_{H\max}$ which is the typical one for western Central Europe. In contradiction to this breakout direction data are the azimuths of only two available earthquake *P* axes of earthquakes in this nearly aseismic region. One of these is well constraint NE-SW directed (after *Leydecker et al.* [1980] at 52.94°N, 9.95°E, B quality) the other at 52.26°N, 7.71°E is NNE-SSW oriented (after *Hinzen* [1984], C quality). But these earthquake *P* axes are in best agreement with the $S_{H\max}$ directions for the eastward adjoining area. The reason for the differing $S_{H\max}$ directions in different horizons in the western North German plain is not clear. The direction jump of about 90° could be interpreted by small differences in the magnitudes of $S_{H\max}$ and $S_{h\min}$, though the data by *Gross* [1989] (see Table 2) do not confirm this hypothesis. On the other hand, a stress rotation with depth cannot generally be excluded. Due to this ambiguity, the two discussed $S_{H\max}$ directions were sketched as trajectories in Figure 4.

Pannonian Basin and Intra-Carpathians

According to *Horvath and Royden* [1981] and *Royden et al.* [1982] and Pannonian basin is characterized by Neogene E-W extension and, probably, N-S compression (continuing recently with minor activity however the main phase of extension was in the Badenian, 16.5–30 Ma). This deformation occurred along mostly NE and NW trending sets of conjugate shear: NE trending faults exhibit sinistral offsets, while NW trending faults are dextral. But the $S_{H\max}$ directions mostly available for the margin of the basin do not reflect such a simple stress state characterized by N-S compression and E-W extension. At first glance the $S_{H\max}$ directions seem to scatter considerably. We tentatively interpret these puzzling $S_{H\max}$ orientations as indicating a radial pattern of trajectories around the Pannonian basin. On the other hand, such a radial pattern could be brought into agreement with the extensional regime within the basin as discussed below.

The approximately radial pattern of trajectories around the Pannonian basin implies E-W compression for the intra-Carpathian region east of the basin. This E-W direction is also the dominating orientation of *P* axes of crustal earthquakes in Romania. Some scattering $S_{H\max}$ directions occur in the Vrancea region, at the junction of East and South Carpathians.

Two earthquakes *P* axes are available for the region east of the Carpathian belt (in Figure 2 the two most eastward ones in Romania) which is part of the southwesternmost part of the East European platform. These two *P* axes are NE-SW trending. This is the same direction which follows when the trajectories in Figure 4 would be extrapolated into the region eastward of the Tornquist-Teisseyre line (compare Figure 4). In the Dinarides, SW of the Pannonian basin, the compression is N-S trending, and when approaching the Pannonian basin, it bends to NE-SW.

The pattern of stress-generating plate tectonic forces acting on the eastern intra-Carpathians seems to be rather

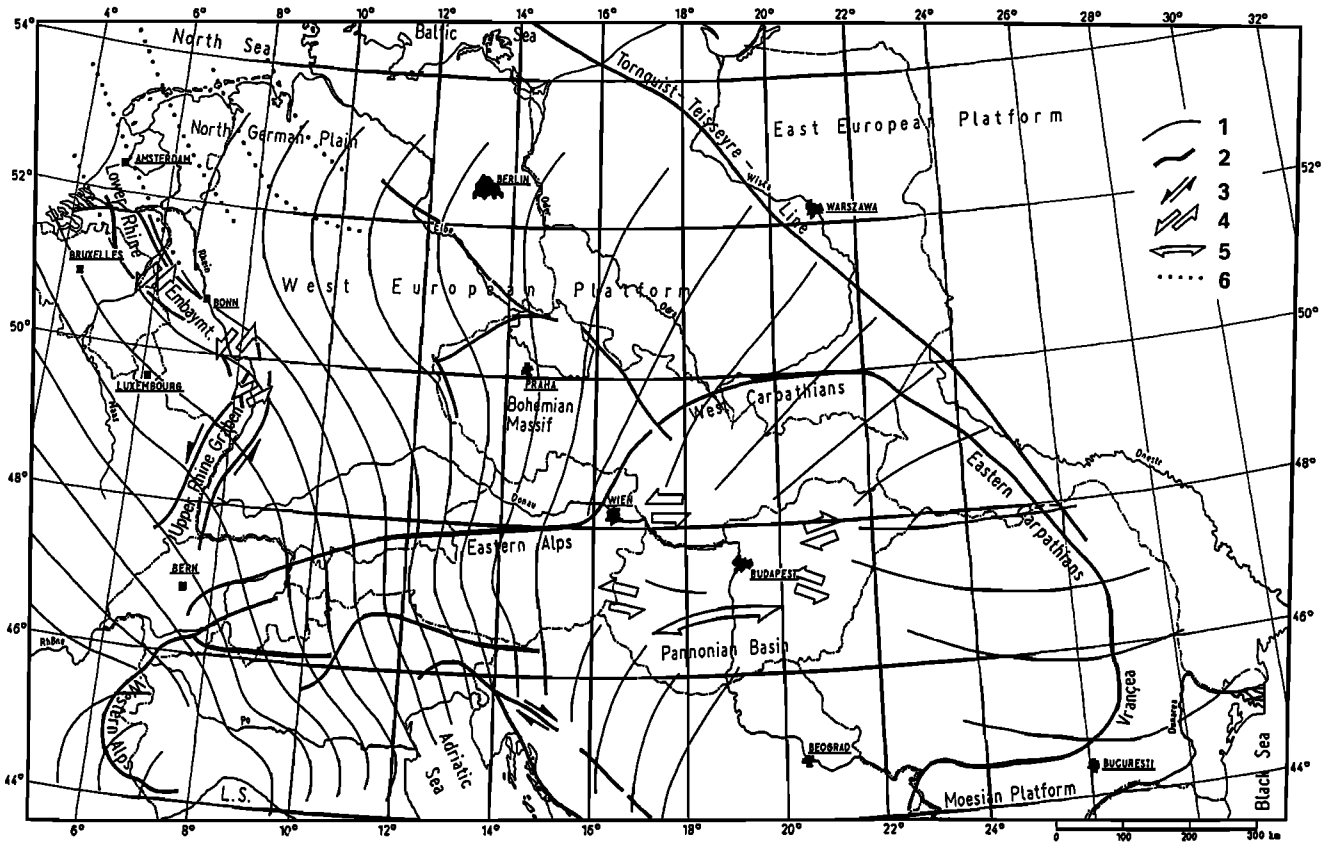

Fig. 4. Stress pattern in Central Europe in a broader sense. 1, trajectories of $S_{H\max}$ representative for the consolidated crust or for the seismogenic depth range; 2, selected first order tectonic faults; 3, sense of shear motion; 4, extensional tectonics with active shearing [*Balla*, 1984]; 5, zone of concentric extension [Balla, 1984]; 6, $S_{H\max}$ trajectories after borehole breakouts and hydraulic fracturing in the sedimentary cover of the western North German plain.

complicated. It is beyond the scope of this paper to give a detailed discussion on the complex tectonism of the Balkan area. We only mention a few of the components which could possibly contribute to the observed crustal stress field in the southeastern part of our study area. The push from the south, that is, of the African plate northward, is probably modulated and perhaps dominated by several secondary plate tectonic motions: (1) *Müller* [1984] suggests that the counterclockwise rotation of the Apennine peninsula is still continuing. This is based on paleomagnetic evidence and focal mechanisms of earthquakes in the Central Alps which show predominantly left-lateral movements. This counterclockwise rotation of Italy would result in a component of horizontal compression with an orientation normal to the coast line of the Adriatic Sea, i.e., a NE-SW direction. (2) The thermal anomaly of the Pannonian basin (due to thermal processes in the upper mantle) could be consistent with the extension within the basin. Appropriate forces have to be responsible for this extension within the plate, especially when the plate is surrounded by compressional push.

The different single extensional features within the Pannonian basin can be connected to several resulting directions of extension. They are depicted in Figure 4 according to the interpretation by *Balla* [1984]. Regardless what physical mechanisms act in the mantle beneath the basin or at the single extensional features they should probably contribute to additional compression components at the margin of the basin. In the eastern part, for example, they could form an additional eastward directed push. More data are needed to discuss if or to which extent the apparent radial stress pattern around the Pannonian basin (Figure 4) could be explained in such a way. (3) Relatively high intermediate-depth seismic activity in 70–140 km in the Vrancea region, as well as crustal earthquakes, indicate active tectonism. The continent-continent collision in the East Carpathians apparently has brought active subduction to a standstill. The mechanism of the intermediate-depth earthquakes reveal the existence of an approximately vertical slab (to depth of 140 km) with a downdip component of extension. This subducted slab has been interpreted by *Fuchs et al.* [1979] to have become separated from the lithosphere in the Vrancea region. Without repeating the details of their interpretation, they conclude that the net downward flow in the upper mantle within a low-velocity zone (40–70 km depth) allows continuing continent-continent collision in the relatively local Vrancea region. Hence drag forces related to this continuing collision could produce additional compressive forces in the crust acting normal to the front of the Carpathians. Furthermore, it is likely that the continent-continent collisional forces at the SE margin of the Carpathians are influenced by the plate tectonic motions east of the African plate, in particular the northward drift of the Arabian plate.

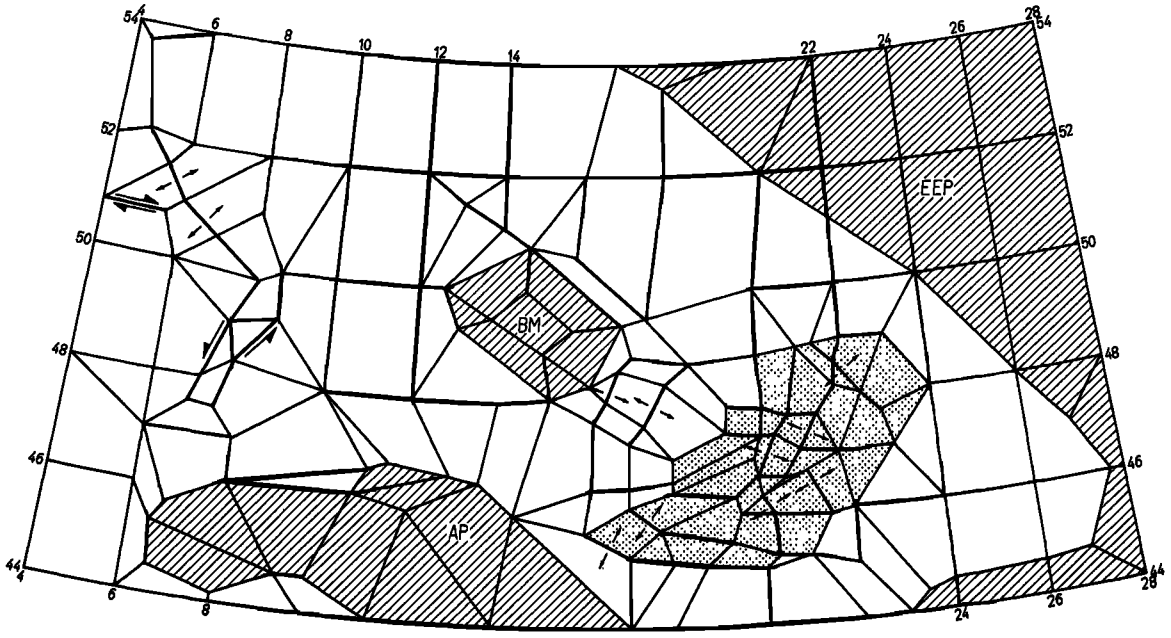

Fig. 5. Finite element mesh for the area under study with the underlying structural and tectonic implications. Different hatching indicates the possibility to introduce varying crustal rigidities (e.g., reduced rigidity (dotted) for the Pannonian basin or increased rigidity for the Adriatic promontory (hatched)). AP, Adriatic promontory; BM, Bohemian massif; EEP, East European platform.

4. Finite Element Modeling

Finite Element Model

At the outset we want to state that the following finite element approach is intended to represent a first-order approximation to explain the observed stress pattern in terms of $S_{H\max}$ trajectories. The stress field within the study region is calculated using a two-dimensional (2-D) finite element technique assuming an elastic plate with nonuniform values of the Young's modulus and Poisson's ratio. This 2-D modeling is indeed a simplified approach, but several arguments favor such a simplification, at least for such first-order approximation: (1) A 3-D modeling would require the introduction of very poorly known boundary conditions at the bottom of the elastic part of the Earth's lithosphere (which occurs at a mean depth of about 25 km within the study area). (2) A ductile lower crust beneath the elastic layer, probably characterized by hydrostatic stress conditions, could contribute to a partial decoupling of the stresses in the upper elastic layer from the ductile one and supports the concept of treating the elastic part separately. (3) Although viscous drag at the base of the plates has necessarily to be neglected in a 2-D modeling, we feel, this seems not to be so important (at least for a first-order approximation), since the drag force plate (proportional to velocity) must be very low for the Eurasian plate which is hardly moving in an absolute reference frame [*Minster and Jordan*, 1978].

The approximation of the spherical surface of the western part of the Eurasian plate by an assembly of isoparametric membrane elements has been carried out in two steps. In the first step the finite element mesh for the region concerned (Central Europe in a broad sense) was constructed (Figure 5). The study region covers the area from 4°E to 28°E and from 44°N to 54°N. An assembly of rectangular elements with a size of 2° × 2° was the starting configuration for the grid. This rectangular net was later specified to accommodate tectonic features.

First, the grid was modified to permit assignment of varying rigidities for different tectonic units, for example, the possibility of increased stiffness for stable blocks such as the Adriatic promontory, the Eastern European platform, and the Bohemian massif and the possibility of reduced stiffness within the Pannonian basin. This differentiation follows from constraints of contrasts in heat flow [*Cermak*, 1979], of structural features, and of the probable role of these units in the tectonic processes. However, areas with geothermal anomalies and an extensional tectonic regime are not necessarily characterized by a decreased strength of the lithosphere [*Shudofsky et al.*, 1987]. As discussed below, our modeling also did not indicate significantly better fit between the observed and calculated stress field for reduced stiffnesses in the thermally active areas. Only a very slight or even no reduction provided the best fit to the observed stress patterns. In addition, some of the elements were designed to reflect the geometry of major tectonic features; however, in the current modeling these features were not utilized.

The principle of our approach was to start with a homogeneous plate where all the above mentioned features do not play any role. Stepwise, the influence of several of these features was analyzed. As will be described below, not all the above possible model refinements were required to explain or to simulate sufficiently the observed $S_{H\max}$ pattern. Figure 6 shows the plate tectonic scheme for the western Eurasian plate. It was the basis for extending the finite element mesh out to the boundaries of the plate (Figure 7). For this larger area the option of introducing differing rigidities was allowed; the regions with potential rigidity contrasts include the remaining parts of the Adriatic prom-

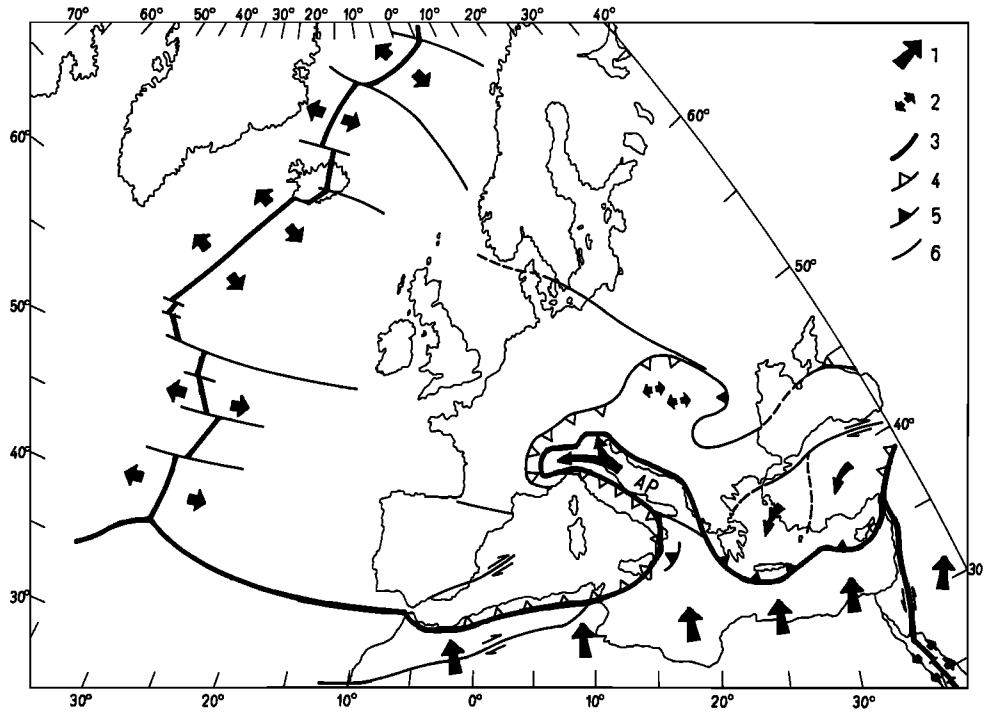

Fig. 6. Plate tectonic scheme of the western part of the Eurasian plate; 1, direction of vector of motion relative to Europe and/or assumed main acting forces at the plate boundary; 2, extensional tectonic regime; 3, main plate boundaries; 4, subduction; 5, thrust and collision; 6, other first order faults with sense of shear motion; AP, Adriatic promontory (mainly after *Horvath* [1984], *Rotstein* [1985], *Letouzey* [1986], and *Weijermars* [1987]).

ontory and the East European platform, as well as regions in the western and eastern Mediterranean, including parts of Turkey, which are characterized by high heat flow and an extensional regime. The same caveat stated above regarding the lack of significant reduced rigidity in high heat flow areas also holds here.

These above described model specifications lead to a strongly irregular finite element pattern. But as will be

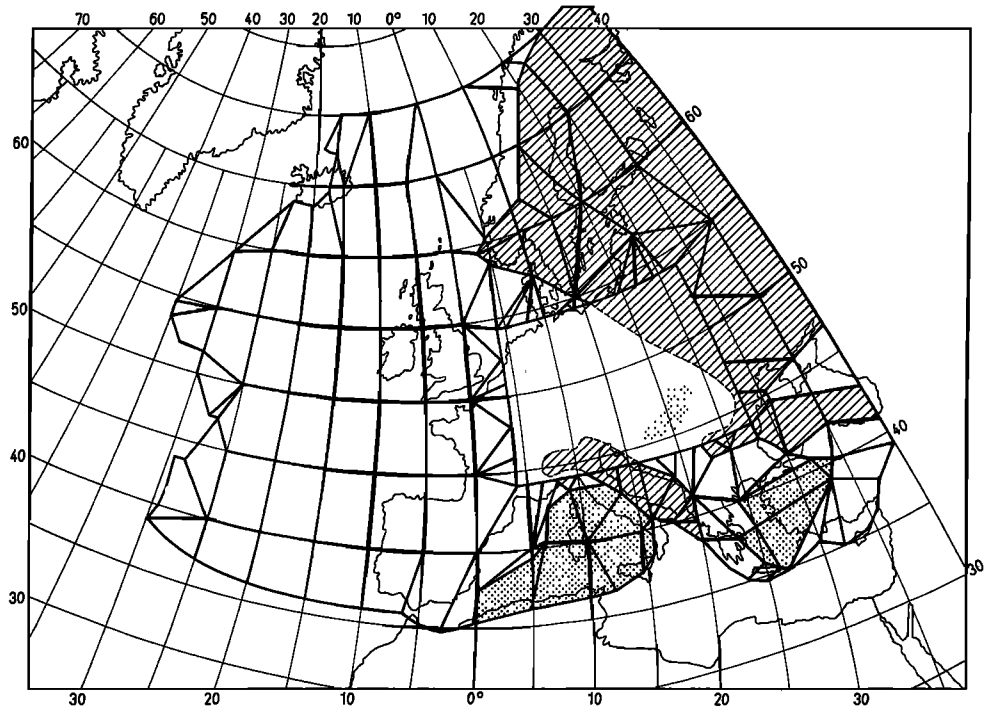

Fig. 7. Finite element mesh for the western Eurasian plate except the region which is shown in Figure 5 (omitted area). Different hatching denotes areas where varying rigidities can be introduced.

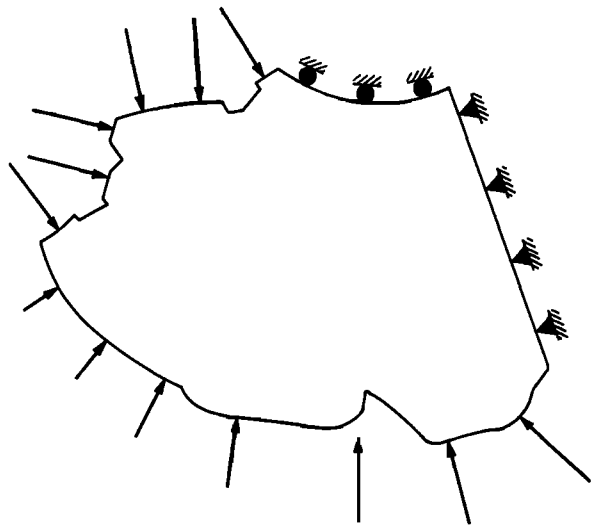

Fig. 8. Distribution of net boundary forces acting on the plate. Different kind of net resistive forces are indicated at 70°N and at 40°E. The length of the arrows schematically reflects the magnitude relations of the forces at the plate boundaries.

shown, only a few of this modeled features were actually required for a sufficient simulation. When no variations of elastic parameters and internal boundaries are used in the model, it is equivalent with a homogeneous and regularly subdivided one.

The northern and eastern boundaries of the mesh were chosen at 70°N and 40°E. These boundaries were assumed to be a sufficient distance from the study area so that edge effects could be ignored (Figure 5). The boundary at 40°E is consistent with the suggestion that there is decoupling between the western and eastern parts of the Eurasian plate [*Molnar et al.*, 1973]. The Adriatic promontory is assumed to be part of (coupled to) the African plate. With such a model the observed stress pattern around the Alps could easily be simulated by appropriate arrangement of the boundary load along the northern tip of this indenter. Alternately, with the model presented, it is shown that completely passive stress generation from the African plate through the Adriatic promontory could explain the observed stress pattern simply by introduction of increased rigidity for the promontory.

The restriction in our computations on $S_{H\max}$ orientations for a reference thickness of the elastic lithosphere could be considered an advantage since rheological conditions of oceanic and continental lithosphere are not fully understood until now. Also, estimates of the equivalent elastic thickness of the lithosphere vary considerably [e.g., *Quinlan and Beaumont*, 1984; *Stephenson*, 1984]. Tests indicate that variation of the Young's modulus E from 1 to 100 GPa in our modeling does not cause substantial changes of the calculated $S_{H\max}$ orientations. *Cloetingh and Wortel* [1986] used a Young's modulus $E = 70$ GPa in a similar finite element study for the Indo-Austalian plate with an assumed reference thickness of 100 km. We adopted for our first-order approximation of the $S_{H\max}$ directions a variation of E of 70 ± 30 GPa with a mean $E = 50$ GPa and a Poisson's ratio of 0.3. Attempts to incorporate the rheological effects rigorously in a deterministic way must await more progress in determining the rheology of the Eurasian lithosphere.

Force Modeling

The plate tectonic scheme of the western Eurasian plate (Figure 6) indicates the main plate boundary forces considered to model the state of stress in the seismogenic depths range of the study area. The two primary sources of stress are (1) the force resulting from the northward motion of Africa relative to Europe (continental convergence force) and (2) the ridge-push force from the central and northern segments of the Mid-Atlantic Ridge. The dominant northward directed motion of Africa with respect to Europe has continued during the last 45 m.y. [e.g., *Biju-Duval et al.*, 1977]. A compilation of velocity vectors of the regional geokinematics in the Mediterranean region [e.g., *Drewes*, 1984] clearly shows the northward movement of Africa in the order of about 1 cm/yr. Unfortunately, geodetic observations of the displacement of points in North Africa with respect to Europe were lacking until now. A spreading velocity of 2.2 cm/yr was determined for the North Atlantic [*Minster and Jordan*, 1978; *Dietrich et al.*, 1989]. For symmetrical spreading, the relative eastward shift of Eurasia would be half of this value, which is approximately equal to the estimated northward motion of Africa.

Collisional resistance forces generally act normal to plate boundaries (Figures 6 and 8). In case of pronounced protrusions of boundaries (as in southernmost Italy), the forces due to rigidity of the promontory may more likely act in the general direction of relative plate convergence rather than following the irregular shape of boundaries as depicted in Figure 8. The North Atlantic ridge force was assumed to be normal to the ridge (see Figure 8). The 2-D technique used for this first-order approximation does not allow the consideration of stress effects due to topography, buoyancy, and basal drag (also see preceding section).

Currently, the only stress parameter of the Earth's crust which is available with sufficient reliability and in sufficient quantity is the orientation of $S_{H\max}$. Owing to that fact, our modeling was restricted to a regional interpretation of azimuths of $S_{H\max}$. This restriction to the calculation of direction values considerably simplifies the force modeling because the problem of proper introduction of sufficiently reliable absolute values of forces acting on the plate can be ignored. (A thorough discussion and application of absolute forces was given by *Cloeting and Wortel* [1986] in connection with stress modelings of the Indo-Australian plate.)

The restriction to calculations of $S_{H\max}$ orientations, presented as an integral value per each finite element and based on relative forces acting on the plate, means that the magnitude of all acting forces can be scaled up or down by the same factor. The ratio between the relative magnitudes of North Atlantic ridge push and of the collisional force acting in the south of the model was determined by trial-and-error modelings. The test criterion was the well-established NW-SE directed $S_{H\max}$ orientation in western Central Europe. The starting model was a ratio between both forces of one. This fit the test criterion very well. Moderate variations of this ratio did not change the goodness of fit much. For simplicity and because the test showed little difference with varying ratios of the ridge push to the convergence force, we adopted the simple starting model. This would coincide with the above mentioned nearly equivalent velocities of the plate motions. But this does not mean that the ratio of acting forces could be deduced simply from the ratio of observed

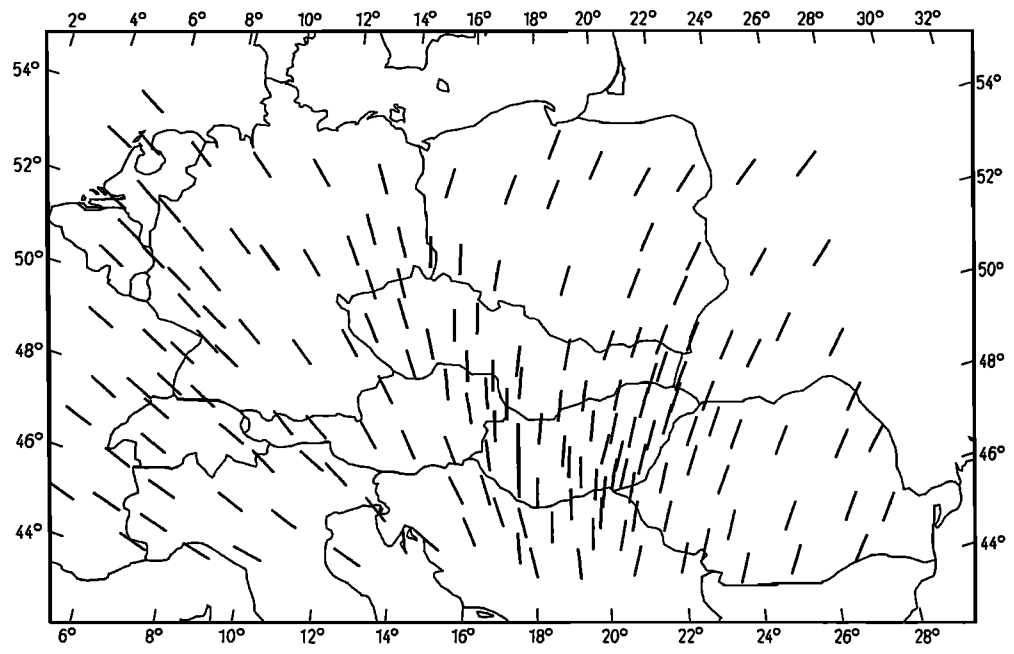

Fig. 9. Calculated $S_{H\max}$ directions as integral values per each finite element according to the boundary load displayed in Figure 8 and a uniform elastic plate with a Young's modulus E = 50 GPa (starting model).

velocities of motions. The relative velocities at plate boundaries are the result from all the forces affecting the two plates involved.

The observed spreading rates along the boundaries of the African plate suggest a counterclockwise rotation of this plate [*Minster and Jordan*, 1978]. Concerning the collisional forces of the African plate on the Eurasian plate, this would require for our simple modeling increasing the values of the applied forces from east to west as indicated in Figure 8. It is shown below that the approximately equivalent relative magnitudes of both primary forces promptly lead to the general pattern of observed $S_{H\max}$ directions.

Several secondary sources of stress mentioned above in the preceding section on stress trajectories were also considered, these include (1) a possible continent-continent collision of second order at the SE margin of the Carpathians, (2) probable thermal processes in the upper mantle of the Pannonian basin, and (3) possible anisotropies of elastic parameters (also see preceding paragraph).

Procedure and Results

As discussed previously, several model parameters or boundary conditions had to be adopted because most of the elastic parameters and boundary line forces necessary for the modeling are not known with the desired precision. Only the geometrical boundaries seem to be well constrained by geological, tectonical, and geophysical facts. However, this trial-and-error like approach within the given limits of model parameters may be useful as a first-order approximation in simulating the observed $S_{H\max}$ directions.

Starting position of our modeling was a homogeneous elastic plate (E = 50 GPa) under boundary load, as described previously, from the North Atlantic Ridge and from the northward push of Africa (see Figure 8). The calculated horizontal stress field in terms of the directions of $S_{H\max}$ (as integral value per each element) is displayed, for the region especially concerned here, in Figure 9. Already, with these most simple model assumptions, the general observed stress pattern (Figure 4) could be simulated quite well. The calculated $S_{H\max}$ orientations (Figure 9) show the well-known dominating NW-SE direction in western Central Europe. The bending of the $S_{H\max}$ trajectories into NE-SW direction in eastern Central Europe (see Figure 4) is also predicted with the starting homogeneous model. This result leads us to the conclusion that an increased rigidity for the East European platform (leading to an intensified bending of stress trajectories) is not required. The relation of the absolute values of $S_{h\min}$ to $S_{H\max}$ of this model is in no position smaller than 0.6. In regions where $S_{h\min}$ and $S_{H\max}$ have nearly the same values, already relatively small local anomalies of elastic parameters could result in a rotation, or a 90° switch of the $S_{H\max}$ direction.

The starting model shows especially in three areas a significant nonconformity between observed (Figures 2 and 4) and first computed (Figure 9) orientations of $S_{H\max}$. These are the western Alps, the Pannonian basin, and the western margin of the Bohemian massif. Stepwise, the congruence between observations and simulations was improved by refining the boundary conditions. The first refinement of the modeling involved the introduction of increased rigidity for the Adriatic promontory (E = 100 GPa). The justification for this increased rigidity was discussed in the preceding section. This increase in rigidity leads to the observed fanlike pattern of the $S_{H\max}$ trajectories perpendicular to the arc of the Western Alps (see Figures 3 and 4). A more detailed finite element mesh in this region would display this feature more pronounced. A more accurate modeling of this feature would require a 3-D approach in order to simulate the subsiding cold and dense lithosphere root [*Müller*, 1984]. These effects were simulated in our 2-D model as a first-order approximation by the increased Young's modulus of the Adriatic promontory.

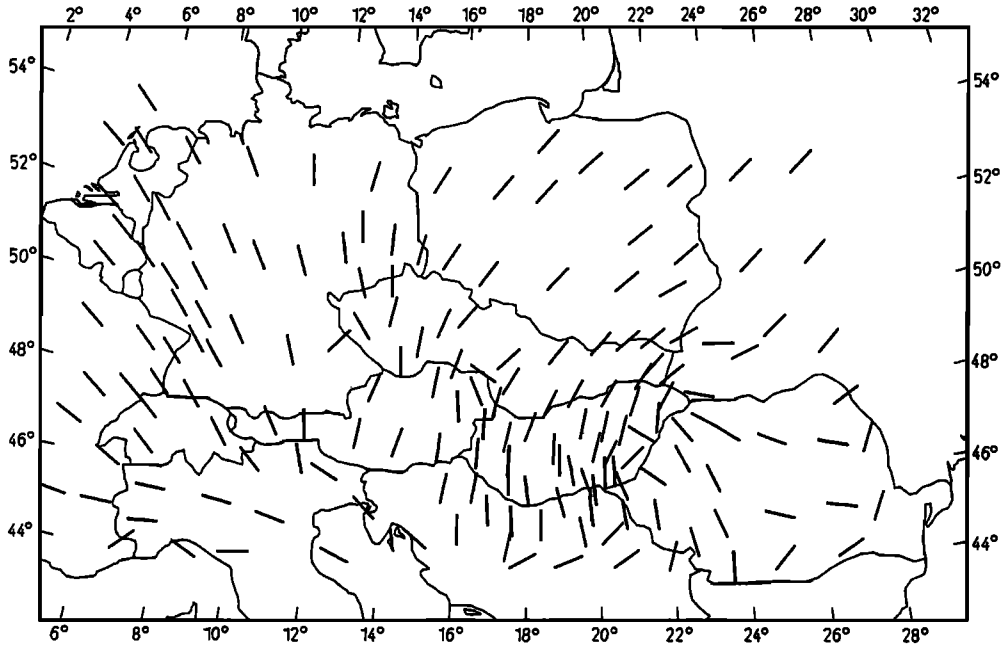

Fig. 10. Calculated $S_{H\max}$ directions as in Figure 9 but with the following model specifications to simulate localized sources of stress: increased rigidity (E = 100 GPa) for the Adriatic promontory and the Bohemian massif (see Figures 5 and 7), slightly decreased rigidity (E = 40 GPa) for the Pannonian basin and additional line forces acting eastward from the Panonian basin and at the southeastern Carpathians (for explanations, see text).

Additional model calculations were carried out with different degrees of decreased rigidity for the high heat flow, extensional regions (i.e., the Pannonian basin, the western and eastern Mediterranean). In particular, the effects of such a decrease in rigidity was studied for the Pannonian basin. However, none of the models with reduced rigidity produced the observed radial pattern, in fact the effect was just the opposite; that is, this model type produced NE-SW trending trajectories as they would develop around a hole in a plate. The admissible reduction of east was only from 50 to 40 GPa. This result is in agreement with the observations and considerations of *Shudofsky et al.* [1987], showing that the East African rift exhibits considerable strength down to lower crustal levels.

The starting homogenous model (Figure 9) predicted NNE-SSW $S_{H\max}$ directions in the intra-Carpathians east of the Pannonian basin. However, the observed $S_{H\max}$ orientations in this region are dominately E-W directed (Figures 2 an 4). The only way we found to model the E-W directed compression in the eastern intra-Carpathians was to consider the effects of the previously described possible continent-continent collision force at the SE margin of the Carpathians as well as possible compression components connected with the extension in the Pannonian basin (see section on stress trajectories and on force modeling). The amount and direction of forces which could be assumed to act in the Vrancea region, the junction between East and South Carpathians, have also been discussed previously. According to geological constraints [*Balla*, 1984] we assume that a possible compression originated from the extensional regime of the Pannonian basin could act, for example, from the east margin of the basin to the east and from the SW margin to the SW. The relative forces were adopted to be of the same order as those acting at the Vrancea region. Such a model leads to a WNW-ESE $S_{H\max}$ direction for the eastern intra-Carpathians (see Figure 10) which is very similar to the observed E-W orientation of $S_{H\max}$ in that region. Such a model would be throughout plausible, but we have to concede that it is based on several not well-constrained assumptions for the intra-Carpathians.

The numerous well-established NW to WNW oriented $S_{H\max}$ values derived for the most western part of the Bohemian massif (see Figure 2 and *Grünthal et al.* [1990]) are not well simulated, with our starting model showing NNW orientations of $S_{H\max}$. Furthermore, the NE-SW orientations of $S_{H\max}$ in the southern part of the Bohemian massif and in eastern Austria (Figure 2) are not at all consistent with the starting model which predicted NNW-SSE orientations. Previously, a possible increased rigidity for the Bohemian massif was mentioned. This is based on geologic and geophysical evidence characterizing the Bohemian massif as a stable independent block of continental crust, a typical example of a "central massif", that is, an ancient Proterozoic core encompassed by younger material which was affected by several episodes of tectonism. This geological-tectonical point of view of the Bohemian massif as a stable block caused us to assign it with an increased rigidity (E = 100 GPa). The resulting $S_{H\max}$ directions within as well as along the margins of this stable block fit the observed orientations reasonably well (Figure 10). These are the final model modifications considered in our preliminary trial-and-error approach. Better constrained attempts and 3-D modelings incorporating depth depending features must await progress in describing the rheological structure of the lithosphere in the region studied.

5. Conclusions

The data, their generalization in form of trajectories and the attempts for interpretation presented here, represent a

progress report on the analysis of the state of crustal stress in Central Europe, emphasizing the eastern part. Analysis of the $S_{H\max}$ direction data of the studied region permits the following conclusions:

1. Practically all observations on $S_{H\max}$ orientations could be fitted visually into a generalized and homogenized pattern of stress trajectories.

2. This pattern consists of a regionally uniform broad-scale stress field which is superimposed by more localized sources of tectonic stress.

3. The regional stress pattern is characterized by $S_{H\max}$ orientations which seem to rotate gradually from the well-established and well-known NE-SE direction in western Central Europe to the direction NE-SW in the eastern part and even farther to E-W in the SE part of the studied region.

4. More localized sources of tectonic stresses are prevailing in the western Alps as the already well-known fanlike stress pattern normal to the arc of the Western Alps, in and around the Pannonian basin as an obvious radial pattern, and less pronounced in and around the Bohemian massif which seems to deflect the $S_{H\max}$ directions.

5. The observed stress pattern could be simulated by two-dimensional, steady state, elastic finite element calculations on the basis of both net plate boundary forces acting on the western part of the Eurasian plate and more localized features which were reduced on rigidity anomalies for the Adriatic promontory and the Bohemian massif. This simple 2-D approach gives very reasonable results. A more complex 3-D modeling would require introduction of more boundary conditions (elastic parameters, boundary forces, and a physical description of the characteristics at the bottom of the model) which are only barely feasible to date. Therefore we conclude that the applied trial-and-error like approach may be useful to date as a first-order approximation in simulating the crustal stress field in the regional scale.

6. A balance of North Atlantic ridge push and pushes resulting from the northward drift of the African plate fits sufficiently well the observed broad-scale stress field.

7. Attempts to simulate the stress field in the eastern intra-Carpathians require the introduction of plausible additional line forces possibly to be explained by the extensional tectonic regime in the Pannonian basin and due to local active tectonism in the Vrancea region and/or influences of collisional forces of the Arabian plate. However, especially this part of the modeling requires additional stress and strain data. With the presented approach it is not intended to represent a final modeling; rather it is intended to stimulate further studies on this subject.

Acknowledgments. We are indepted to all the workers whose research efforts have produced the data used in our study. The manuscript was greatly improved by constructive remarks of anonymous critical reviewers. Especially, we very much appreciate the highly useful suggestions of M. L. Zoback, Associate Editor for this issue. We want to thank L. Ahorner for allowing us to use his diagram showing orientations of different types of stress indications. Contribution 1847 of the Central Institute for Physics of the Earth.

REFERENCES

Ahorner, L., Present-day stress field and seismotectonic movements along major fault zones in Central Europe, *Tectonophysics*, *29*, 233–249, 1975.

Ahorner, L., The general pattern of seismotectonic dislocations in Central Europe as the background for the Liège earthquake on November 8, 1983, in *Seismic Activity in Western Europe*, edited by P. Melchior, pp. 41–56, D. Reidel, Norwell, Mass., 1985.

Ahorner, L., and H. Murawski, Erdbebentätigkeit und geologischer Werdegang der Hunsrück-Südrand-Störung, *Z. Dtsch. Geol. Ges.*, *126*, 63–82, 1975.

Ahorner, L., and R. Pelzing, Seismotektonische Herdparameter von digital registrierten Erdbeben der Jahre 1981 und 1982 in der westlichen Niederrheinischen Bucht, *Geol. Jahrb., Reihe E*, *26*, 35–63, 1983.

Ahorner, L., and G. Schneider, Herdmechanismen von Erdbeben im Oberrhein-Graben und seinen Randgebirgen, in *Approaches to Taphrogenesis*, edited by H. J. Illies and K. Fuchs, pp. 104–117, Schweizerbart, Stuttgart, Germany, 1974.

Ahorner, L., H. Murawski, and G. Schneider, Seismotektonische Traverse von der Nordsee bis zum Apennin, *Geol. Rundsch.*, *61*, 915–942, 1972.

Ahorner, L., B. Baier, and K. P. Bonjer, General pattern of seismotectonic dislocation and the earthquake generating stress field in Central Europe between the Alps and the North Sea, in *Plateau Uplift*, edited by K. Fuchs et al., pp. 187–197, Springer-Verlag, New York, 1983.

Antonini, M., Variations of the focal mechanisms of 1985/86 Western Bohemia swarm events—correlation with spatial distribution of foci and suggested geometry of faulting, in *Proceedings of a Workshop on Induced Seismicity and Associated Phenomena, Liblice, March 14–18, 1988*, vol. I, pp. 250–270, Czechoslovak Academy of Sciences, Prague, 1988.

Balla, Z., The Carpathian loop and the Pannonian Basin: A kinematic analysis, *Geophys. Trans. Budapest*, *30*(4), 313–353, 1984.

Baumann, N. H., and H. J. Illies, Stress field and strain release in the Rhenish Massif, in *Plateau Uplift*, edited by K. Fuchs et al., pp. 177–186, Springer-Verlag, New York, 1983.

Baumgärtner, J., F. Rummel, and Chu Zhaotan, Wireline hydraulic fracturing stress measurements in the Falkenberg Granite Massif, *Geol. Jahrb., Reihe E*, *39*, 83–99, 1987.

Becker, A., Messung und Interpretation oberflächennaher in situ-Spannungen am Südost-Ende des Oberrheingrabens und im Tafeljura, Ph.D. thesis, Univ. Karlsruhe, Germany, 1985.

Becker, A., and S. Paladini, In situ-Spannungen in Nord- und Mitteleuropa, *Schr. Angew. Geol. Karlsruhe*, *10*, 1–63, 1990.

Becker, A., P. Blümling, and W. H. Müller, Rezentes Spannungsfeld in der zentralen Nordschweiz, *Tech. Rep. NAGRA 84-37*, 35 pp., Natl. Genoss. für die Lagesung Radioaktiv. Abfälle, Baden, Germany, 1984.

Biju-Duval, B., J. Dercourt, and X. Le Pichon, From the Tethys Ocean to the Mediterranean Seas: A plate tectonic model of the evolution of the Western Alpine system, in *International Symposium of Structural History of Mediterranean Basins, Split (Yugoslavia)*, edited by B. Biju-Duval and L. Mondadert, pp. 44–72, Technip, Paris, 1977.

Blümling, P., In-situ-Spannungsmessungen in Tiefbohrungen mit Hilfe von Bohrlochrandausbrüchen und die Spannungsverteilung in der Kruste Mitteleuropas und Australiens, Ph.D. thesis, Univ. Karlsruhe, Germany, 1986.

Blümling, P., K. Fuchs, and P. Schneider, Orientation at the stress field from breakouts in a crystalline well in a seismic active area, *Phys. Earth Planet. Inter.*, *33*, 250–254, 1983.

Bonjer, K.-P., D. Gelbke, B. Gilg, D. Rouland, D. Mayer-Rosa, and B. Massinon, Seismicitiy and dynamics of the Upper Rhinegraben, *J. Geophys.*, *55*, 1–12, 1984.

Cagnetti, V., V. Pasquale, and S. Polinari, Focal mechanisms of earthquakes in Italy and adjacent regions, *Rep. RT/AMB 76*, 4 pp., Com. Naz. Energ. Nucl., Rome, 1976.

Carniel, P. and K.-H. Roch, In situ-Gebirgsspannungsmessungen im Felbertal, Österreich, *Riv. Ital. Geofiz. Sci. Aff.*, *3*, 233–250, 1976.

Cermak, V., Heat flow map of Europe, in *Terrestrial Heat Flow in Europe*, edited by V. Cermak and L. Rybach, pp. 3–40, Springer-Verlag, New York, 1979.

Cloetingh, S., and R. Wortel, Stress in the Indo-Australian plate, *Tectonophysics*, *132*, 49–67, 1986.

Cox, J. W., Long axis orientation in elongated boreholes and its correlation with rock stress data, *Trans. SPWLA Annu. Logging Symp.*, *24th*, 1–17, 1983.

Dietrich, R., G. Gendt, and F. Barthelmes, Geodynamic research using Lageos laser ranging data at the Central Institute for Physics of the Earth Potsdam, paper presented at the IAG General

Meeting, Int. Assoc. of Geod., Edinburgh, Scotland, Aug. 3–12, 1989.

Dorel, J., et al., Focal mechanism in metropolitan France and Lesser Antilles, *Ann. Geophys.*, *1*, 299–306, 1983.

Drewes, H., Models for monitoring regional geokinematics in the Alpine-Mediterranean region, *Ann. Geophys.*, *2*, 235–238, 1984.

Fuchs, K., et al., The Romanian earthquake of March 4, 1977: Aftershocks and migration of seismic activity, *Tectonophysics*, *53*, 225–247, 1979.

Gangl, G., Seismotectonic investigations of the western part of the inner Alpine Pannonian Basin (eastern Alps and Dinarides), in *Proceedings of XIV General Assembly European Seismological Commission, Trieste, Sept. 16–22, 1974*, pp. 409–410, Nationalkomitee für Geodasie und Geophysik, Berlin, 1975.

Gasparini, C., G. Iannaccone, and R. Scarpa, Fault-plane solutions and seismicity of the Italien peninsula, *Tectonophysics*, *117*, 59–78, 1985.

Gibowicz, S. J., and A. Cichowicz, Source paarameters and focal mechanism of mining tremors in the Nowa Ruda coal mine in Poland, *Acta Geophys. Pol.*, *34*(3), 215–232, 1986.

Gibowicz, S. J., B. Guterch, H. Lewandowska-Marciniak, and L. Wysokinski, Seismicity induced by surface mining: The Belchatow, Poland, earthquake of 29 November 1980, *Acta Geophys. Pol.*, *30*(3), 193–219, 1982.

Gibowicz, S. J., J. Niewiadomski, P. Wiejacz, and B. Domanski, Source study of the Lubin, Poland, mine tremor of 20 June 1987, *Acta Geophys. Pol.*, *37*(2), 111–132, 1989.

Greiner, G., In-situ stress measurements in southwest Germany, *Tectonophysics*, *29*, 265–274, 1975.

Greiner, G., and J. H. Illies, Central Europe: Active or residual tectonic stress, *Pure Appl. Geophys.*, *115*, 11–26, 1977.

Gross, U., Untersuchungen zum Gebirgsspannungszustand in der Altmark, research report, Inst. für Bergbausicherheit, Leipzig, Germany, June 1989.

Grosser, H., and W. Köhler, Focal plane solutions of the main events during the earthquake swarm 1985/86 in western Bohemia/Vogtland, in *Proceedings of a Workshop on Induced Seismicity and Associated Phenomena, Liblice, 14–18 March 1988*, vol. II, pp. 49–64, Czechoslovak Academy of Sciences, Prague, 1988.

Grünthal, G., and D. Stromeyer, Stress pattern in Central Europe and adjacent areas, *Gerlands Beitr. Geophys.*, *95*, 443–452, 1986.

Grünthal, G., V. Schenk, A. Zeman, and Z. Schenkova, Seismotectonic model for the earthquake swarm 1985/86 in the focal area Vogtland/West Bohemia, *Tectonophysics*, *174*, 369–383, 1990.

Hermann, W., F. Kohlbeck and A. E. Scheidegger, In situ stress measurements in highly fractured rock at Hüttenberg Austria, *Mitt. Oesterr. Geol. Ges.*, *76*, 161–166, 1983.

Hiller, W., Das oberschwäbische Erdbeben am 27, Juni 1935, Württbg, *Jahrb. Stat. Landeskunde*, *1934/35*, 209–226, 1936.

Hinzen, K.-G., Nordrhein-Westfalen, Teutoburger Wald, in *Erdbeben in der Bundesrepublik Deutschland 1981*, pp. 20–22, Bundesanstaet für Geowissenschaften und Rohstoffe, Hannover, Germany, 1984.

Horvath, F., Neotectonics of the Pannonian basin and the surrounding mountain belts: Alps, Carpathians and Dinarides, *Ann. Geophys.*, *2*, 147–154, 1984.

Horvath, F., and L. Royden, Mechanism for the formation of the intra-Carpathian basins: A review, *Earth Evol. Sci.*, *1*(3/4), 307–316, 1981.

Illies, J. H., H. Baumann, and B. Hoffers, Stress pattern and strain release in the Alpine foreland, *Tectonophysics*, *71*, 157–182, 1981.

Jimenez, M. J., and N. Pavoni, Focal mechanisms of recent earthquakes 1976–1982 and seismotectonics in Switzerland, *Veroeff. Zentralinst. Phys. Erde Potsdam*, special issue, 77–84, 1984.

Knoll, P., Analyse der Gebirgsspannungen in Bergbaurevieren der DDR, *Freib. Forschungsh. C*, *349*, 61–73, 1979.

Kohlbeck, F., In situ-Spannungsmessungen im Tertiärbecken von Frohnsdorf, *BHM Berg Hüttenmaenn. Monatsh.*, *124*(8), 367–376, 1979.

Kohlbeck, F., K.-H. Rock, and A. E. Scheidegger, In situ stress measurements in Austria, *Rock Mech., Suppl. 9*, 21–29, 1980.

Kohlbeck, F., K.-H. Rock, and A. E. Scheidegger, In situ-Spannungsmessungen im Gleinalmtunnel, *BHM Berg Hüttenmaenn. Monatsh.*, *126*(4), 134–140, 1984.

Kotas, A., Structural evolution of the Upper Silesian cole basin (Poland), paper presented at 10th International Congress on Carbon Stratigraphy, Madrid, Sept. 12–19, 1983.

Kraft, K., In situ-Gebirgsspannungsmessungen im Grund- und Deckgebirge von Oberfranken/Nordost-Bayern, dissertation, Univ. of Bayreuth, Germany, 1984.

Laubscher, H. P., The arcs of the Western Alps and the Northern Apennines: An updated view, *Tectonophysics*, *146*, 67–78, 1988.

Letouzey, J., Cenozoic paleo-stress pattern in the Alpine Foreland and structural interpretation in a platform basin, *Tectonophysics*, *132*, 215–231, 1986.

Leydecker, G., M. Steinwachs, D. Seidl, R. Kind, J. Klussmann, and W. Zerna, Das Erdbeben vom 2. Juni 1977 in der norddeutschen Tiefebene bei Soltau, *Geol. Jahrb., Reihe E*, *18*, 3–18, 1980.

Martinetti, S., and S. Ribacchi, In situ-stress measurements in Italy, *Rock Mech., Suppl. 9*, 31–47, 1980.

Minster, J. B., and T. H. Jordan, Present-day plate motions, *J. Geophys. Res.*, *83*, 5331–5353, 1978.

Mjakisev, V., Untersuchung des Gebirgsspannungszustandes im Südostteil der DDR, Ph.D. thesis, Bergakademie, Freiberg, Germany, 1983.

Molnar, P., T. J. Fitch, and F. T. Wu, Fault plane solutions of shallow earthquakes and contemporary tectonics in Asia, *Earth Planet. Sci. Lett.*, *19*, 101–112, 1973.

Monus, P., L. Toth, and T. Zsiros, Focal mechanism solutions of Central European earthquakes, poster presented at the XXIth General Assembly, Eur. Seismol. Comm., Sofia, Aug. 23–27, 1988.

Müller, B., K. Fuchs, L. Mastin, S. Gregersen, N. Pavoni, O. Stephanson, C. Ljunggren, and M. L. Zoback, Regional patterns of tectonic stress in Europe, *J. Geophys. Res.*, this issue.

Müller, St., Dynamic processes in the Alpine arc, *Ann. Geophys.*, *2*, 161–164, 1984.

Neugebauer, H. J., and E. Tobias, A study of the Echzell/Wetterau earthquake of November 4, 1975, *J. Geophys.*, *43*, 751–760, 1977.

Oncescu, M. C., On the stress tensor in Vrancea region, *J. Geophys.*, *62*, 62–65, 1987.

Oncescu, M. C., and C. J. Trifu, A large seismic sequence on April 27–29, 1986 in Vrancea foredeep, Romania, St. Cerc, *Stud. Cescetari Geol. Geofiz.*, *25*, 88–97, 1987.

Pavoni, N., Zur Seismotektonik des Westalpenbogens, *Vermess. Photogramm. Kulturtech.*, *3/4*, 185–187, 1975.

Pavoni, N., Crustal stresses inferred from fault-plane solutions of earthquakes and neotectonic deformation in Switzerland, *Rock Mech., Suppl. 9*, 63–68, 1980*a*.

Pavoni, N., Comparison of focal mechanism of earthquakes and faulting in the Helvetic zone of Central Valais, Swiss Alps, *Eclogae Geol. Helv.*, *73*, 551–558, 1980*b*.

Pavoni, N., Regularities in the pattern of major fault zones of the earth and the origin of arcs, in *The Origin of Arcs*, edited by F.-C. Wezel, pp. 63–78, Elsevier Scientific, New York, 1986.

Pavoni, N., and E. Peterschmitt, Das Erdbeben von Juerre vom 21, Juni 1971 und seine Beziehungen zur Tektonik des Faltenjura, in *Approaches to Taphrogenesis*, edited by J. H. Illies and K. Fuchs, pp. 322–329, Schweizerbart, Stuttgart, Germany, 1974.

Philip, H., Tectonique recente et sismicite de la France: caracteristiques geodynamiques, in Evolutions geologiques de la France, *Mem. BRGM*, *107*, 42–50, 1980.

Pilarski, I., Neotektonik S-Teil DDR, *Res. Rep. ZO 0600-7530-1339*, Zentralinst. für Phys. der Erde, Potsdam, Germany, 1988.

Poljak, M., Neotectonic investigations in the Pannonian basin based on satellite images, *Adv. Space Res.*, *4*(11), 139–146, 1984.

Polonic, G., Neotectonic activity at the eastern border of the Pannonian depression and its seismic implications, *Tectonophysics*, *117*, 109–115, 1985.

Pospisil, L., V. Schenk, and Z. Schenkova, Relation between seismoactive zones and remote sensing data in the West Carpathians, in *Proceedings of 3rd International Symposium on the Analysis of Seismicity and Seismic Risk, Liblice Castle, June 17–22, 1985*, vol. I, pp. 256–263, Czechoslovak Academy of Sciences, Prague, 1985.

Quinland, G. M., and C. Beaumont, Appalachian thrusting, lithospheric flexure and the Paleozoic stratigraphy of the eastern interior of North America, *Can. J. Earth Sci.*, *21*, 973–996, 1984.

Radu, C., The tectonic stress and tectonic motion direction in Romania, in *Proceedings of Seminar on Seismic Zoning Maps, Skopje 1975*, vol. I, pp. 84–100, UNESCO, Paris, 1976.

Ritsema, A. R., The earthquake mechanisms of the Balkan Region, *UNDP Proj. REM/70/172*, UNESCO, 1974.

Rotstein, Y., Tectonics of the Aegean block: Rotation, side arc collision and crustal extension, *Tectonophysics*, *117*, 117–137, 1985.

Royden, L., F. Horvath, and B. C. Burchfiel, Transform faulting, extension, and subduction in the Carpathian Pannonian region, *Geol. Soc. Am. Bull.*, *93*, 717–725, 1982.

Rummel, F., and H. J. Alheid, Hydraulic fracturing stress measurements in SE Germany and tectonic stress pattern in Central Europe, in *Proceedings of the U.S.–Yugoslav Research Conference on Intra-Continental Earthquakes, Ohrid, Yugoslavia, 1979*, pp. 33–66, Institute of Earthquake Engineering and Seismology, Skopje, Yugoslavia, 1980.

Rummel, F., and J. Baumgärtner, Spannungsmessungen im östlichen Bereich der Südwestdeutschen Scholle, *Res. Rep. RUB-7084408-82-3*, Bochum, 1982.

Rummel, F., and J. Baumgärtner, Hydrofrac Spannungsmessungen in den geothermischen Erkundungsbohrungen des kontinentalen Tiefbohrprogramms im Schwarzwald und in der Oberpfalz, research report, Ger. Sci. Found., Berlin, 1987.

Rummel, F., J. Baumgärtner, and H. J. Alheid, Hydraulic fracturing stress measurements along the eastern boundary of the SW-German block, in *Proceedings of Workshop on Hydraulic Fracturing Stress Measurements, Dec. 2–5, 1981*, pp. 3–17, National Academy Press, Washington, D. C., 1983.

Schmedes, E., Bayerische Molasse, in *Erdbeben in der Bundesrepublik Deutschland 1981*, pp. 25–26, Bundesanstalt für Geowissenschaften und Rohstoffe, Hannover, 1984.

Schmedes, E., Alpen und Molasse, in *Erdbeben in der Bundesrepublik Deutschland 1982*, p. 45, Bundesanstalt für Geowissenschaften und Rohstroffe, Hannover, 1987.

Schneider, G., Erdbeben und Tektonik in Südwest-Deutschland, *Tectonophysics*, *5*, 459–511, 1967.

Schneider, T., Bohrlochrandausbrüche in norddeutschen Bohrungen und ihre Beziehung zum regionalen Spannungsfeld-Beobachtung und Theorie, diploma thesis, Geophys. Inst. Univ. Karlsruhe, Germany, 1985.

Shudofsky, G. N., S. Cloetingh, S. Stein, and R. Wortel, Unusually deep earthquakes in East Africa; Constraints on the thermomechanical structure of a continental rift system, *Geophys. Res. Lett.*, *14*, 741–744, 1987.

Slunga, R., P. Norman, and A.-C. Glans, Baltic shield seismicity: The results of a regional network, *Geophys. Res. Lett.*, *11*, 1247–1250, 1984.

Stephenson, R., Flexural models of continental lithosphere based on the long term decay of topography, *Geophys. J. R. Astron. Soc.*, *11*, 385–413, 1984.

Thurm, H., P. Bankwitz, E. Bankwitz, and G. Harnisch, Rezente horizontale Deformationen der Erdkruste im Südteil der DDR, *Petermanns Geogr. Mitt.*, *4*, 281–304, 1977.

Vyskocil, P., Dynamics of the Bohemian Massif, *Veroeff. Zentralinst. Phys. Erde*, *81*(III), 156–159, 1985.

Vyskocil, P., Horizontal recent tectonic deformations in Western Bohemia, in *Earthquake Swarm 1985/86 in Western Bohemia*, pp. 388–390, Czechoslovak Akademy of Sciences, Geophysical Institute, Prague, 1987.

Weijermars, R., A revision of the Eurasian-African plate boundary in the western Mediterranean, *Geol. Rundsch.*, *76*, 667–676, 1987.

Wolter, K., Untersuchung der in situ-Spannung, Residualspannung und der Mikroriβsysteme in Graniten Süddeutschlands, Ph.D. thesis, Univ. Karlsruhe, Germany, 1987.

Zahradnik, J., V. Vavrycuk, J. Jansky, and J. Zednik, Focal mechanisms of selected events of West Bohemia earthquake swarm 1985/86 constrained by *P*-wave amplitudes, in *Proceedings of Workshop on Induced Seismicity and Associated Phenomena, Liblice, March 14–18, 1988*, pp. 271–289, Czechoslovak Academy of Sciences, Prague, 1988.

Zoback, M. L., State of stress and modern deformation of the northern Basin and Range Province, *J. Geophys. Res.*, *94*, 7105–7128, 1989.

Zoback, M. L., First- and second-order patterns of stress in the lithosphere: The World Stress Map project, *J. Geophys. Res.*, this issue.

Zoback, M. L., and M. D. Zoback, Faulting patterns in north central Nevada and strength of the crust, *J. Geophys. Res.*, *85*, 275–284, 1980*a*.

Zoback, M. L., and M. D. Zoback, State of stress in the conterminous United States, *J. Geophys. Res.*, *85*, 6113–6156, 1980*b*.

Zoback, M. L., et al., Global patterns of tectonic stress, *Nature*, *341*(6240), 291–298, 1989.

G. Grünthal and D. Stromeyer, GeoForschungsZentrum Potsdam, D-1561 Potsdam, Germany.

(Received January 16, 1990;
revised September 5, 1990;
accepted July 22, 1991.)